Measurement-efficient optical wavemeters

P. Potuluri, M. E. Gehm, M. E. Sullivan, and D. J. Brady

Fitzpatrick Center for Photonics and Communications Systems,
Duke University, Durham, NC 27708 USA
dbrady@duke.edu

http://www.disp.duke.edu

Abstract: We describe a method for efficiently determining the wavelength of a monochromatic source and provide an experimental proof-of-concept. The photomeasurement efficiency for a wavemeter can be written as $\eta(N,q) = (1 + \log_q N)/m$, where N is the number of spectral channels, q is the number of distinguishable output levels per photodetector, and m is the actual number of photomeasurements made. An implementation is developed that achieves a theoretical efficiency of $\eta(N,q) = 1$. The proof-of-concept experiment achieves efficiencies $\eta = O(1)$, where the deviation from theory is attributable to well-known optical effects and should be correctable in future versions.

OCIS codes: (120.6200) Spectrometers and spectroscopic instrumentation; (220.4830) Optical systems design.

References and links

1. J.J. Snider, "Laser Wavelength meters," Laser Focus **18**(5), 55-61 (1982).
2. J.J. Snyder and T.W. Hansch, "Laser wavemeters," in *Topics in Applied Physics: Dye Lasers,* F.P. Schafer, ed. (Springer-Verlag, Berlin, 1990), pp.201-219.
3. J.-P. Monchalin, M.J. Kelly, J.E. Thomas, N.A. Kurnit, A. Szoke, F. Zernike, P.H. Lee, and A. Javan, "Accurate laser wavelength measurement with a precision two-beam scanning Michelson interferometer," Appl. Opt. **20,** 736-757 (1981).
4. P.J. Fox, R.E. Scholten, M.R. Walkiewicz, and R.E. Drullinger, "A reliable, compact, and low-cost Michelson wavemeter for laser wavelength measurement," Am. J. Phys. **67,** 624-630 (1999).
5. M-L. Junttila, B. Stahlberg, E. Kyro, T. Verijola and J. Kauppinen, "Fourier transform wavemeter," Rev. Sci. Instrum. **58,** 1180-1184 (1987)
6. D. Steers, W. Sibbett and M.J. Padgett, "Dual-purpose, compact spectrometer and fiber-coupled laser wavemeter based on a Wollaston prism," Appl. Opt. **37,** 5777-5781 (1998).
7. D. Du and F. Hwang, *Combinatorial group testing and its applications, vol. 12 of Series on Applied Mathematics* (World Scientific, Singapore, 2000).
8. U. Gopinathan, D.J. Brady and N.P. Pitsianis, "Coded apertures for efficient pyroelectric motion tracking," Opt. Express **11,** 2142-2152 (2003), http://www.opticsexpress.org/abstract.cfm?URI=OPEX-11-18-2142.
9. D.J. Schroeder, *Astronomical Optics* (Academic, San Diego, Calif. 1987).
10. C. Papaliolios, P. Nisenson, and S. Ebstein, "Speckle imaging with the Papa detector," Appl. Opt. **24,** 287-292 (1985).

---

1. Introduction

An optical wavemeter estimates the operating wavelength of a quasi-monochromatic signal. With the advent of tunable laser sources and their increased use in spectroscopy and communication systems, the need for compact and convenient wavemeters has emerged.

Numerous designs [1, 2] have been proposed over the years, most of them based on interferometric concepts. The most commonly used is a scanning-Michelson interferometer [3, 4, 5]. In this design, a stable laser with well-characterized wavelength is used as a frequency reference. The reference and the unknown source are injected into a Michelson interferometer and their interference fringes are simultaneously detected on different detectors. The relative lengths of the interferometer arms are varied while the number of fringes is counted for both the reference and unknown source. The ratio of the two fringe counts gives the ratio of the two wavelengths. The scanning nature of this design typically leads to relatively fragile instruments. There are robust static wavemeter designs, most notably those based on Wollaston prisms [6]. These designs interfere the unknown source with a transversely shifted version of itself, resulting in a spatial fringe pattern which is recorded on a detector array. However, in this case, the resolution of the wavemeter is limited by the number of pixels on the detector array, as it sets a limit on the highest spatial frequency that can be detected in the interferogram. Large, high resolution detector arrays are expensive, especially in the infrared spectral region.

In general, the existing wavemeter designs have been optimized for resolution. However, there are cases where resolution is not the key design parameter. In coarse dense-wavelength-division-multiplexing (DWDM) communication systems, the required resolution is such that simple dispersion spectrometers are sufficient as long as the resulting wavemeter is compact, portable, robust, and inexpensive. The wavelengths of interest, however, require detectors of indium-gallium-arsenide (InGaAs). InGaAs detector arrays are very expensive, so a successful design will minimize the number of detector elements required.

In this paper, we describe a method to determine the wavelength of a laser source within N spectral channels, using just $O(\log(N))$ detectors instead of the $O(N)$ detectors required in the case of a traditional dispersion based spectrometer.

We are able to reduce the number of measurements because the quasi-monochromatic source has a highly-constrained input state. The spectral density of such a source is of the form $S(\lambda) = I_0 \delta(\lambda - \lambda_0)$, where δ is the Dirac delta-function and I_0 and λ_0 are the only unknowns. The unknown λ_0 is restricted to a particular spectral range and and the function of the wavemeter is to identify which particular spectral channel the source occupies. We use group testing techniques to minimize the number of measurements required.

Group testing has generally been applied to the analysis of discrete objects, such as coins, weights or chemical samples [7]. Recently, our group applied the methodology to the problem of identifying which of N possible physical locations is occupied by an object while making only $\log_2(N)$ measurements [8]. Here we extend the approach from physical locations to spectral channels and combine multiplex sensing and group testing in the spectral domain to efficiently identify the unknown spectral channel.

We can define the system *photomeasurement efficiency* $\eta(N,q)$ as

$$\eta(N,q) = \frac{\chi(N,q)}{m}. \tag{1}$$

Here N is the number of spectral channels, q is the number of distinguishable output states of a single photodetector, $\chi(N,q)$ is the theoretical minimum number of photomeasurements required under these conditions, and m is the actual number of photomeasurements made. Equation 1 can also be viewed as the ratio of the number of possible input states to the number of possible measurement states. Perfect efficiency occurs when there is an *one-to-one mapping* between the input states and the measurement states of the sensor.

The photomeasurements can be performed at multiple detectors (*e.g.* a traditional dispersion spectrometer), or at different times (*e.g.* a Fourier transform spectrometer), or at a combination of the two (*e.g.* a scanning-Michelson wavemeter). In these traditional systems, the number of photomeasurements greatly exceeds the theoretical minimum ($m \gg \chi(N,q)$), so $\eta(N,q) \ll 1$.

Below, we describe a design for an optical wavemeter that, in theory, achieves $\eta(n,q) = 1$. Our proof-of-concept implementation achieves $\eta(N,q) \simeq O(1)$, with the deviation from theory due to well known physical effects that can be corrected for in future implementations.

2. Theory

For an input state of the form given above, the function of a wavemeter can be alternatively described as determining which single spectral channel, of the N available spectral channels, is occupied. This problem can easily be solved by a *binary search* algorithm, although of a slightly different form than normal.

In the traditional binary search, we ask a series of questions of the form "Is the occupied channel in the first- or second-half of the range a to b?" Based on the answer, we redefine a and b to be the endpoints of the range identified in the previous question and ask again. It can be shown that this will uniquely identify which of the N channels is occupied after $\log_2(N)$ questions. This approach, however, is adaptive in that the questions we ask depend on the answers we received previously.

If we instead ask questions of the form "Is the occupied channel in an odd- or even-half (quarter, eighth, sixteenth, *etc.*) of the full spectral range?," we can ask all of the questions simultaneously and still uniquely determine the occupied channel in $\log_2(N)$ questions. To express the questions mathematically, we number the channels from 0 to $N-1$, designate the index of the unknown occupied channel as j, and write

$$
\begin{aligned}
d_1 &= \left\lfloor \frac{j}{2} \right\rfloor (\mathrm{mod}\,2) \\[6pt]
d_2 &= \left\lfloor \frac{j}{2^2} \right\rfloor (\mathrm{mod}\,2) \\[6pt]
d_3 &= \left\lfloor \frac{j}{2^3} \right\rfloor (\mathrm{mod}\,2) \\[6pt]
&\;\;\vdots \\[6pt]
d_m &= \left\lfloor \frac{j}{2^m} \right\rfloor (\mathrm{mod}\,2),
\end{aligned}
\tag{2}
$$

where $\lfloor\;\rfloor$ is the floor operator (round down to nearest integer) and *mod* indicates that this calculation is to be performed *modulo* 2. If N is a power of 2, we have completely identified the value of j when $m = \log_2(N)$.

If our detectors are binary (only capable of detecting the presence/absence of light), then this is the best we can do at reducing the required number of photomeasurements. However, if we can distinguish q different output levels from the photodetectors, then we can generalize our approach from a binary search to a q-ary search. The mathematical form of the measurements becomes in this case

$$
\begin{aligned}
d_1 &= \left\lfloor \frac{j}{q} \right\rfloor (\mathrm{mod}\,q) \\[6pt]
d_2 &= \left\lfloor \frac{j}{q^2} \right\rfloor (\mathrm{mod}\,q) \\[6pt]
d_3 &= \left\lfloor \frac{j}{q^3} \right\rfloor (\mathrm{mod}\,q) \\[6pt]
&\;\;\vdots \\[6pt]
d_m &= \left\lfloor \frac{j}{q^m} \right\rfloor (\mathrm{mod}\,q),
\end{aligned}
\tag{3}
$$

When $q = 2$, there is no ambiguity about the value of a measurement—either a detector sees light or it does not. But when we use $q > 2$, there can be ambiguity about what value a measurement represents. For this reason, we must add one additional measurement—one that captures the full power of the signal for comparison with the other measured values. Thus, we must in general make $\chi(N,q) = 1 + \log_q(N)$ measurements to fully determine the occupied channel, making the photomeasurement efficiency (Eq. 1)

$$\eta(N,q) = \frac{1 + \log_q(N)}{m}.$$ (4)

As a side benefit, however, the additional measurement allows us to also determine the power in the source. For the remainder of the manuscript, we will use the form of Eq. 4 for all bases.

3. Experimental implementation

Having determined that the theoretical minimum number of measurements is described by a q-ary search, we now turn to trying to implement such a search in hardware, with the hopes of achieving a dramatic gain in photomeasurement efficiency. The key step is producing a wavelength-dependent intensity modulation on the light. Because there are m required measurements, we must have m different intensity codes. As mentioned in the introduction, these codes could be separated sequentially in time, separated spatially on different detectors, or a combination of both. We desire a completely static system, so we choose to implement the m codes on m spatially-separated photodetectors. As a result, our approach is best described as implementing a spatial-spectral-intensity code on the input light.
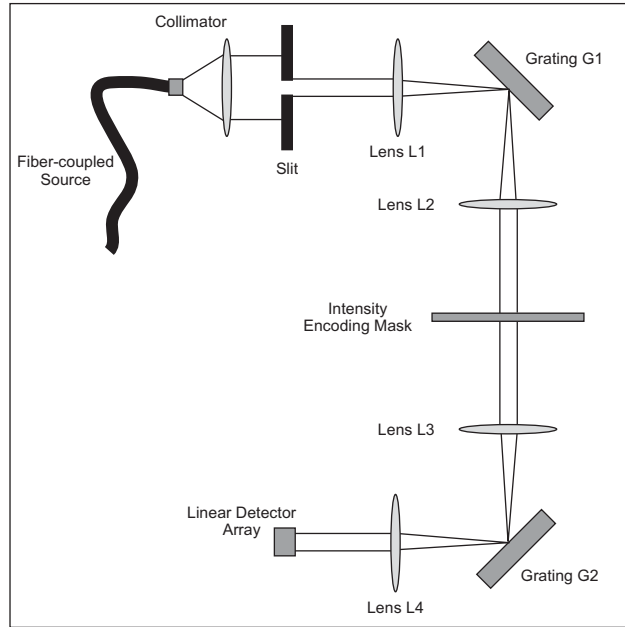

Fig. 1. Physical layout of the wavemeter system.

A physical layout which implements a spatial-spectral-intensity code on the input state is pictured in Fig. 1. The light enters the wavemeter from an optical fiber. The fiber output is collimated and strikes an input slit. The light from the slit passes through lens L1, is diffracted

by grating `G1` and then passes through lens `L2` before striking the intensity encoding mask. The lenses are arranged in a 4-f configuration such that the slit is imaged onto the mask. The presence of the grating causes the image of the slit to vary in horizontal position in proportion to the wavelength of the input light.

The mask is designed with m rows and N columns. The rows correspond to different measurements while the columns correspond to different spectral channels. The light from the slit interacts with only a single column of the mask, becoming encoded with the intensity modulation identifying that particular spectral channel.

The intensity-encoded light then passes through lens `L3`, strikes grating `G2` (which undoes the dispersion introduced by `G1`) and passes through lens `L4` before striking a linear array of m photodetectors. Again, the lenses are arranged in a 4-f configuration, producing an image of the slit (now intensity encoded) on the array of photodetectors. The spectral channel occupied by the source is then uniquely determined by the intensity modulation recorded across the detectors.
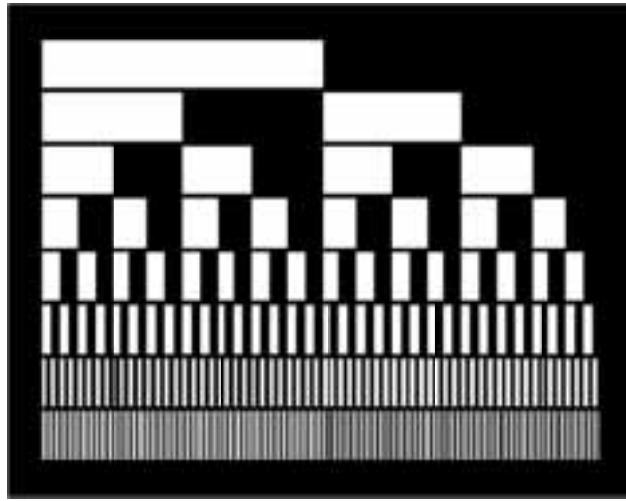

Fig. 2. Mask pattern for binary ($q = 2$) detectors.

With binary detectors, a mask for $N = 256$ channels (and hence $m = 8$ detectors) is shown in Fig. 2. The white regions are completely transparent, while the black regions are completely opaque. Note that this mask does not contain a row that implements the measurement of the total power. This is because there is no ambiguity in detector levels for purely binary detectors. However, as a result, this mask will not allow the determination of the source power.

Implementing the system with detectors of higher dynamic range requires us to modulate the light to a number of intermediate intensity levels. Producing a mask with grayscale transmission levels is more difficult than producing a simple binary-valued mask. As an alternative, we can make use of the finite extent of the photodetectors and modulate the height of the transmissive regions in the mask to achieve intermediate transmission levels. A mask for $N = 256$ spectral channels and quaternary ($q = 4$) detectors is shown in Fig. 3. Again, white indicates completely transparent regions, while black indicates completely opaque regions. As expected, there are five ($m = 1 + \log_4(256)$) distinct rows, including the disambiguation row which simply measures the source power. The period 4 variation in the transmission levels is clearly observable as a modulation in the height of the transmissive regions.

Fig. 3. Mask pattern for quaternary ($q = 4$) detectors.

4. Results and analysis

For diagnostic purposes, we imaged the output plane of the wavemeter rather than letting it strike a linear detector array. A sample image taken using the binary mask of Fig. 2 is shown in Fig. 4. The clear representation of the bit-pattern "10001100" can be seen.
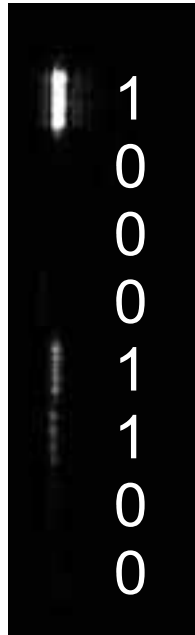

Fig. 4. Detection of the bit-pattern 10001100.

The analysis of the data is done by simulating the presence of a linear array in the detection plane. That is, for each simulated photodetector, we designate a pixel region in the image.

Further, these regions are of identical size and shape, and are regularly spaced along a line. The signal from the photodetector is taken to be the sum of the pixel values in its associated region. The location of these regions are determined at the beginning of the experiment (similar to aligning the photodetector array), and then not moved during the course of the experiment.

In the binary case, the photodetector signals are simply thresholded to convert the data into a bit pattern. For masks with $q > 2$, the values are first divided by the photodetector signal of the calibration row, and then thresholded into the q different levels.

We used an HP 8168E tunable laser source to test the wavemeter. The optical system was arranged such that the spatial channel widths on the masks in Figs. 2 and 3 were equivalent to a 1 nm bandwidth. We scanned the laser source from 1470 nm to 1570 nm in 1 nm increments and recorded the intensity distribution in the output plane. The limitation to a 100 nm scan range was a result of the tunability of our source. The recorded intensity images were processed using the technique described above.
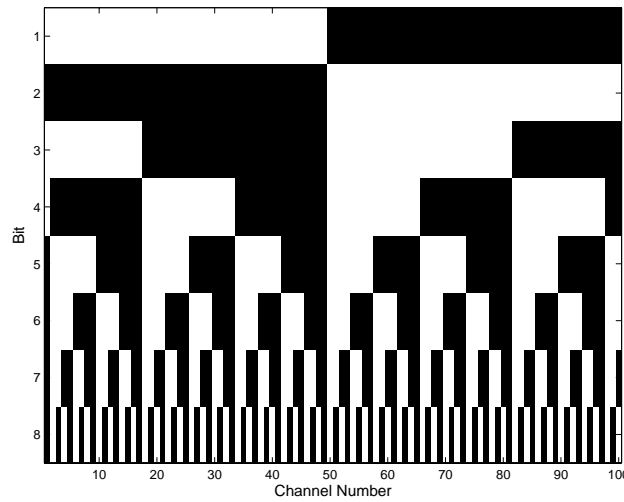

Fig. 5. Expected bit patterns for the binary mask. White indicates "1", black indicates "0."

Each of the 100 channels should generate a different bit pattern when sampled through the masks. The 100 patterns are shown in image form in Fig. 5. Each column represents a different spectral channel, while the rows represent the bit value assigned to each of the individual photodetectors. A white region indicates the bit is a "1" for that spectral channel, while black indicates a "0." The specific details of the pattern depends on where the 100 channels fall on the 256 channel mask. The pattern shown is for the experimental conditions described above. After processing the collected data, we can plot the results in a similar manner. This is done in Fig. 6. The difference between the two plots, and hence the locations of bit errors, is shown in Fig. 7. Similar plots can be generated for the case with $q = 4$. These plots are shown in Figs. 8, 9, and 10. The calibration row has been suppressed from these plots.

Looking at the error plots (Figs. 7 and 10), we see that the errors occur primarily in the lower channel numbers and in the photodetectors which are masked with the highest resolution patterns. We believe that these errors are predominantly caused by the well-known curvature of a slit imaged through a grating [9]. This slight curvature can be seen in Fig. 4. As a result, the light does not interact with a perfectly vertical strip of the mask, falling instead on a gentle arc. As a result, the light (especially in the regions with the highest resolution mask patterns) is sometimes masked as if it is in a neighboring spectral channel. This hypothesis is further
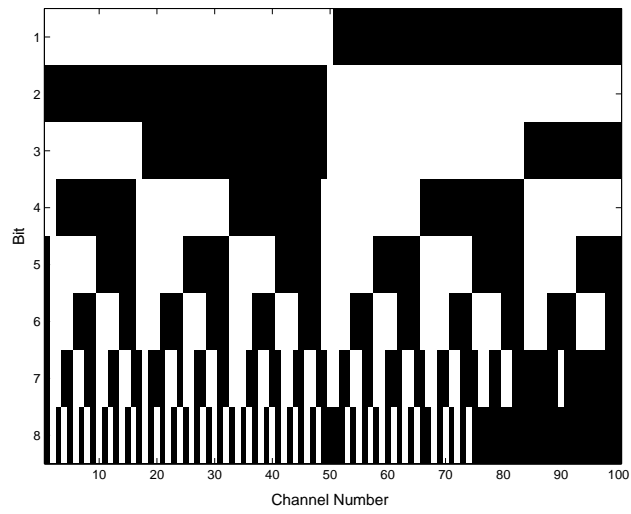
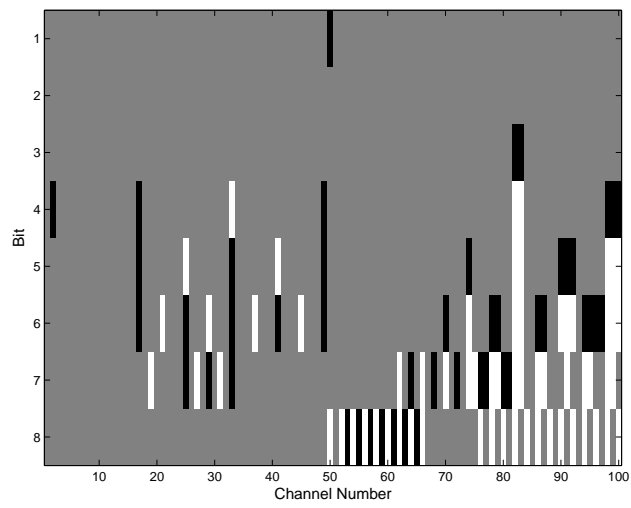Fig. 6. Measured bit patterns for the binary mask. White indicates "1", black indicates "0."

Fig. 7. Bit errors (theory minus measured) for the binary mask. White indicates "1", gray indicates "0", and black indicates "-1."
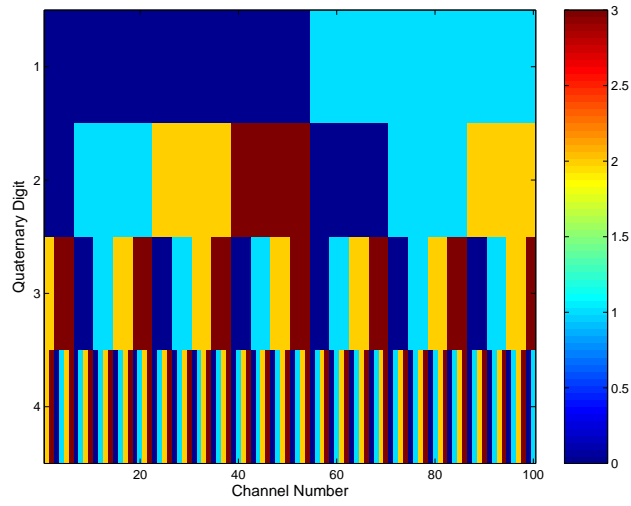
Fig. 8. Expected quaternary digit patterns for the quaternary ($q = 4$) mask. Values are indicated by the colorbar. The calibration row has been suppressed in this image.
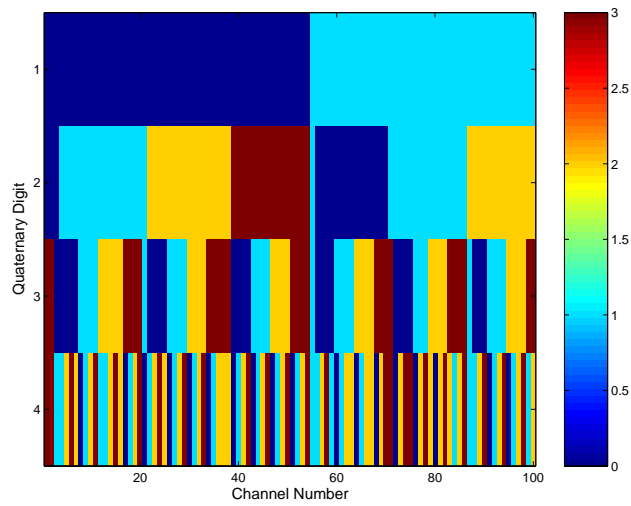

Fig. 9. Measured quaternary digit patterns for the quaternary ($q = 4$) mask. Values are indicated by the colorbar. The calibration row has been suppressed in this image.
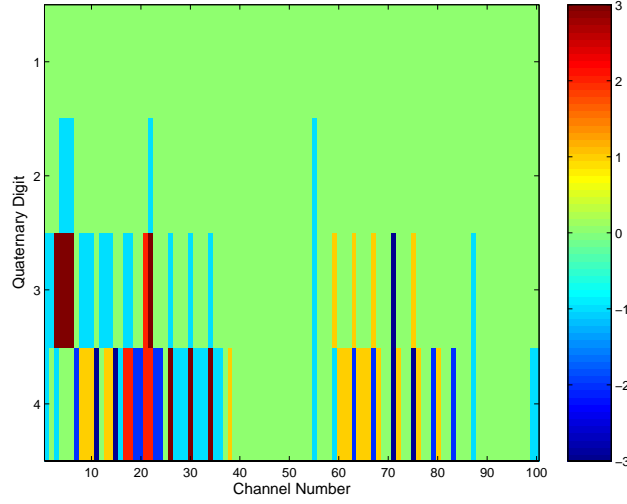
Fig. 10. Errors (theory minus measured) for the quaternary ($q = 4$) mask. Values are indicated by the colorbar. The calibration row has been suppressed in this image.

supported by the fact that the overall structure of the measured results (Figs. 6 and 9) is of the same qualitative form as the theoretical results (Figs. 5 and 8). That is, the measured signals are not random, and tend to show the expected periodicity—they are just sometimes out of phase with the other photodetectors by a channel or two. We should be able to correct for this problem in a future version of the wavemeter by modifying the mask so that it has a slight arc to match the expected curvature of the slit image.

Additionally, a refined version of the wavemeter would most likely not use the binary (or q-ary) search codes described above. These masks were chosen because they most directly demonstrate the logarithmic scaling that is possible in this system and have the appealing quality of converting an occupied spectral channel into the base-q representation of the channel number. This feature, however, requires some neighboring channels to have drastically varying bit-sequences. As a result, small variations in a single q-ary digit can result is channel estimates that are very distant in state-space from the true input state. For this reason, a gray code is probably the best choice for a final implementation. The perfomance of gray code in comparison to binary code has already been demonstrated with the papa detector [10]. The gray code would retain the logarithmic scaling just like the binary code, but ensures that errors in a single q-ary digit produce estimates that are close to the true state.

Overall the performance of the wavemeter is very promising. Clearly we cannot achieve $\eta(N, q) = 1$, as our source can only supply 100 channels and the masks were designed for 256. For the binary mask, this corresponds to a maximum possible value of $\eta_{\max}(100, 2) = (1 + \log_2(100))/8 = 0.96$ (the binary mask does not have a calibration row), while for the quaternary mask it is $\eta_{\max}(100, 4) = (1 + \log_4(100))/5 = 0.86$. With the binary mask we managed to achieve 82 unique intensity codes for an actual value of $\eta_{\exp}(82, 2) = (1 + \log_2(82))/8 = 0.92$. For the quaternary mask, we achieved 84 unique intensity codes for an actual value of $\eta_{\exp}(84, 4) = (1 + \log_4(84))/5 = 0.84$. Both represent better than an order of magnitude increase over conventional spectrometers and wavemeters.

5. Conclusions

This paper has described and demonstrated a technique for building wavemeters which dramatically decreases the number of photomeasurements required for a given number of spectral channels. The initial proof-of-concept experiments described above achieved $\eta(N,q) \simeq O(1)$—an order of magnitude improvement over traditional sensors. The difficulties observed in the experiment are largely a result of the combination of slit curvature and small mask features, and can be corrected in future designs to push the system closer to the theoretical maximum.

Acknowledgments